The BundleExplorer: A Focus and Context Rendering Framework for Complex Fiber Distributions

D. Röttger[1] and D. Merhof[2] and S. Müller[1]

[1]Institute for Computational Visualistics, University of Koblenz-Landau
[2]Visual Computing, University of Konstanz

Abstract
Advanced diffusion imaging enables the reconstruction of complex fiber configurations such as crossings or fannings. However, resulting visualizations often suffer from visual clutter which makes exploration challenging. This paper presents the BundleExplorer as a GPU-based focus and context rendering framework for diffusion data. A combination of a fiber encompassing hull and line rendering is proposed to provide insight into inner-bundle fiber configurations as well as to enable bundle crossing exploration. Visual clutter is reduced and information about the global bundle geometry is provided by using fiber encompassing hulls. At the same time important characteristics, such as individual trajectory courses, which are conventionally neglected when using hull visualizations, are revealed by cutaway techniques and enhanced line renderings. In addition, spatial features, the distance to the fiber hull, as well as functional features, i.e., the degree of anisotropy, are visualized using fiber color encoding. Different cutaway techniques using marker and view-dependent clippings are implemented in order to reveal focus information. Visual enhancements are used to indicate bundle intersections.

Categories and Subject Descriptors (according to ACM CCS): Computer Graphics [I.3.3]: Picture/Image Generation—; Computer Graphics [I.3.7]: Three-Dimensional Graphics and Realism—; Computer Applications [J.3]: Life and Medical Sciences—

1. Introduction

The Brownian motion of water molecules in fibrous material such as muscles or brain white matter is restricted by microstructural barriers and therefore anisotropic. Diffusion imaging is a magnetic resonance imaging (MRI)-based technique which utilizes the directionality of molecular movement and is thereby able to characterize organized tissue. It is a powerful tool for neuro-visualizations since it is a non-invasive technique to gain information about the course and integrity of neuronal pathways in vivo. Applications of diffusion imaging include neuroscience research and brain disorder diagnosis. In fundamental neuroscience, information about activation area connectivity via white matter fibers is crucial. Neuronal connections obtained by diffusion imaging can answer questions about task-related cortical zones. A further application is neurosurgical planning a preoperative stage in which risk-structures are examined and access paths are defined in order to minimize postoperative damages. White matter pathways pose such risk-structures

since cortical activation zones are connected via neuronal fibers; they are responsible for signal transfer and, therefore, enable communication amongst activation zones. As a result, harming connections disables communication and can cause severe patient impairment. Diffusion tensor imaging (DTI) is the widely used technique which represents the acquired signal with a second order tensor. Tractography techniques estimate trajectories using the principal eigenvector of the diffusion tensor. The resulting pathways are considered to approximate fiber courses and are the most common diffusion imaging visualization technique used by clinicians. However, in regions with fanning, kissing or crossing fibers a DTI diffusion profile is unable to adequately model the underlying fiber structure since the Gaussian assumption only supports a single diffusion magnitude within one voxel. Therefore, more sophisticated models were developed, such as high angular resolution diffusion imaging (HARDI), to overcome the limitations of DTI. The huge contribution of HARDI is the ability to resolve complex fiber networks. Line representations resulting from HARDI-based tractog-

raphy approaches are by nature more complex than DTI-based representations and visualizations are commonly cluttered which makes their interpretation cumbersome. Therefore, advanced visualization approaches are required in order to facilitate intuitive exploration of complex white matter distributions. In this paper we apply recent focus and context approaches to HARDI-based fiber representations. Focus and context approaches are well-known in medical visualizations since they provide understanding of the relationship between various structures by emphasizing focus objects within their context. Here, two fiber constitutions have to be distinguished: First, the constitution of a single neuronal bundle is more complex due to fiber fannings and second, fiber pathways may be seen to interweave. In fact, these issues do not occur using DTI-based reconstructions since streamlines do not fan or interfere with each other.

The main contributions of this paper are:

- We introduce the *BundleExplorer* as a focus and context approach for complex diffusion configurations with minimal user interaction.
- *Inner-bundle fiber visualizations* are integrated in the approach to reveal trajectory courses within their global context.
- *Intersecting-bundle visualizations* are proposed in order to extract spatial features and enable an intuitive exploration of crossing fiber pathways.
- Spatial and functional *bundle features* are encoded in illustrative fiber renderings to enhance diffusion data exploration.
- A *GPU-based framework* for cutaway rendering is proposed to facilitate a fast focus and context rendering of white matter pathways and their encompassing hulls.

Resulting visualizations feature both knowledge about intrinsic fiber configurations as well as the global bundle shape.

This paper is organized as follows: Section 2 provides an overview of related work on diffusion data visualization. Section 3 introduces the used dataset as well as applied fiber and hull rendering techniques. The following Section 4 discusses the main contribution of the paper, the *BundleExplorer*, in detail. Implementation issues are addressed in Section 5 followed by results and discussion of the presented approaches in Section 6 and a conclusion in Section 7.

2. Related Work

Related work on the presented visualization issue targets diffusion visualization the reconstruction and representation of diffusion data, as well as focus and context visualizations, to provide an embedded presentation. In addition, illustrative rendering methods are important to enable a discrimination of focus and context objects. Therefore, scientific work related to our approaches will be reviewed in the following.

Diffusion Visualization: The representation of intra-voxel diffusion distributions using a geometry, known as *glyph-rendering*, is the direct visualization of the diffusion scatter pattern within a voxel. A glyph-based visualization of local diffusion tensors was presented by Kindlmann [Kin04]. He used ellipsoids, cuboids, and superquadrics to represent the local shape of the diffusion tensor. In terms of HARDI, a GPU-based ODF glyph rendering was proposed by Peeters et al. [PPvA*09]. These approaches provide a detailed analysis of local diffusion profiles. However, they do not provide understanding of the global tract configuration the course of neuronal fibers. Individual line representations are the output of diffusion data reconstruction algorithms, so called tractography or fiber tracking approaches. Recently, several advanced fiber rendering techniques emerged, which aim at facilitating fiber exploration: Streamtubes are considered to be beneficial in terms of spatial depth perception but at the same time are computationally more expensive. Therefore, view-oriented and tube-like textured triangle strips are frequently used to imitate streamtubes. Merhof et al. [MSE*06] proposed a method using triangle strips and point sprites for white matter tract visualization. An illustrative rendering approach for line data was proposed by Everts et al. [EBRI09]. The authors introduced a depth-dependent halo technique which focuses on tight line bundles while abstracting less organized line configurations. Another illustrative rendering method for diffusion data was presented by Otten et al. [OVW10]. The proposed method visually generates fiber bundles. Hint lines, silhouettes, and contours are used to simultaneously reduce visual clutter and focus on dominant morphological properties. Hull visualizations, which wrap a surface around the reconstructed lines, are of special interest since clinicians are interested in the border of certain neuronal pathways. Therefore, an emerging visualization method for diffusion data is the generation of fiber encompassing hulls [MME*09, ESM*05, NGE*06, VZKL05]. In terms of diffusion data processing, hulls are motivated by the fact that the computed streamlines only approximate the diffusion process within a voxel; the hulls in turn approximate the reconstructed fibers.

Focus and Context Visualization: A focus and context rendering approach for preoperative neurosurgical planning was proposed by Beyer et al. [BHWB07]. The authors introduced a multimodal and high-quality volume visualization approach including cut-out techniques to visualize deep-seated brain structures. A view-dependent skull peeling approach is applied by generating a view-dependent depth mask. Therefore, visualizations of the surgical approach and especially inner brain structures of interest is feasible. Bruckner et al. [BGKG05] introduced a context-preserving volume rendering approach in which a transfer function is used to evaluate parameters such as shading intensity, gradient magnitude, distance to the eye point, as well as previously accumulated opacity in order to determine less important regions and adjust their opacity. Wang et al. [WZMK05]

introduced the *Magic Volume Lens* as a GPU-based focus and context framework for volume data visualization. The proposed approach is based on direct volume rendering and incorporates several lens shapes as well as transition regions between focus and context objects. The here presented methods are strongly influenced by an approach called *ClearView*, as presented by Krüger et al. [KSW06, KF09]. It comprises a GPU visualization framework for texture-based raycasting. The goal is to focus on particular areas while providing vital context information. The authors propose several approaches to automatically define focus areas and cut-outs based on local volume information. Features, such as the curvature or the distance to the viewpoint or a marker, are extracted and define the importance of objects or regions. The introduced approaches were initially designed for volume data but have been adjusted for geometry data. A level of sparseness approach, called importance driven volume rendering, was proposed by Viola et al. [VKG04]. The introduced method aims at emphasizing important structures covered by less important regions by defining a level of sparseness to each structure. By means of compositing, more important structures are visible through less important ones.

Illustrative rendering and emphasis techniques as well as focus and context visualizations have been further investigated for medical datasets, for example by Tietjen et al. [TIP05]. The authors presented an illustrative hybrid rendering approach for medical datasets including a combination of volume, surface, and silhouette rendering. Tietjen et al. showed that the implementation of silhouettes to indicate the context object is appropriate for surgical planning and facilitates spacial perception. Ropinski et al. [RSH05] used volumetric lenses to define cut-out regions within volumetric datasets in order to achieve efficient exploration of datasets for medical diagnosis. These lenses define regions in which rendering styles change, such as from volume rendering to silhouettes. A GPU-based multimodal visualization framework for neurosurgical planning was proposed by Diepenbrock et al. [DPL*11]. The authors integrated fiber rendering in a multi-volume raycaster and encoded uncertainty through less saturated line renderings. Gasteiger et al. [GNBP11] introduced a focus and context approach, the *FlowLens*, for hemodynamic attribute visualization in cerebral aneurysms. Illustrative streamlines provide insight into blood flow within the aneurysm.

3. Diffusion Data and Rendering Techniques

This section introduces the used diffusion dataset as well as visualization methods for focus and context objects. Individual rendering techniques for fibers and the hull are subsequently combined in the *BundleExplorer* for focus and context visualization.

3.1. Dataset

The human brain HARDI dataset is by the courtesy of Poupon et al. [PPAM06]. It comprises 60 slices with a resolution of 128×128 and an isotropic voxel size of $1.875 \times 1.875 \times 2$ mm. The dataset was acquired with a uniform gradient direction scheme with 200 directions and a b-value of 3000 s/mm^2.

3.2. Fiber Reconstruction and Rendering

Reconstruction is performed using the distance-based tractography approach for HARDI presented in [RSM11]. The approach uses a HARDI anisotropy index to differentiate single from multiple fiber orientations and further computes the distances to white matter boundaries during fiber tracking. We applied a geometry shader-based method presented in [RDM12] for streamtube rendering. This approach constructs, similar to the one presented in [MSE*06], view-oriented triangle strips. Information about the neighbors of each vertex of the input line strip is used in combination with the view vector to generate oriented triangle strips. The fragment shader is designed to imitate tubes by color adjustment: if the current fragment should be displayed in black or according to a colormap, which will be introduced in the following. A closeup of the resulting line visualization is displayed in Figure 1.

Figure 1: Tube-like rendering: result of view-vector oriented triangle strips with applied directional color coding for a single fiber.

3.3. Hull Computation and Rendering

The applied hull computation method extends the approach introduced in [MME*09] which consists of the following consecutive steps: volume rasterization, volume filtering, surface extraction, and surface filtering. We include a reference volume, in this case the rasterized fiber volume, in the surface filtering step to further control geometry adjustments. The reference volume acts as a border for adjusting mesh points: during mesh point displacement the rasterized fiber bundle should not be infiltrated. This additional constraint is implemented because it was observed that the hull quickly infiltrates the fibers in complex bundles and is no longer a sufficient approximation.

In order to facilitate spatial understanding, silhouette rendering as well as Phong illumination is applied to hull rendering. Silhouettes are computed by comparing neighboring depth values in the fragment shader.

3.4. Fiber Color Codings

Two additional color mappings are included in the *Bundle-Explorer* besides the conventional directional color coding.

The first approach highlights functional information, the underlying degree of anisotropy. We use the isotropic, single, multiple fiber index (*ISMI*), proposed in [RDMM12b] since it provides a successful differentiation of HARDI diffusion profiles. Isotropic regions are encoded in white, single fiber distributions in yellow, and multiple fiber distributions in red.

The second approach provides spatial information of fibers. In particular, the constitution of fibers within the encompassing hull. The idea is to color the streamtubes according to their distance to the fiber hull. Distances are computed either to the encompassing hull or a certain geometry, such as a second fiber bundle. The fragment shader is used to visually encode the interpolated fiber distance information. The colormap indicates fiber parts in the vicinity of the hull in red and far away regions in white. Figure 2 shows the introduced color codings for inner bundle visualization in combination with a view-dependent bundle cutaway.

4. The *BundleExplorer*

In the following section, we will introduce the main contribution of this paper the *BundleExplorer*.

Objects can be categorized in the following two classes: *focus objects*, objects of interest, and *context objects*, where one object contains all of the others. In the presented approach, fiber pathway representing lines are the focus object and a fiber encompassing hull is the context object. Section 3 introduced the applied rendering styles for fibers and the hull. In the following, we will explain the combination of both renderings in order to provide a combined visualization and thereby facilitate bundle interpretation. Two interesting fiber-bundle conditions have to be distinguished for focus and context rendering: first, *inner-bundle* aspects and second, *intersecting-bundle* aspects. Inner-bundle visualizations consider a fibers with their encompassing hull. Intersecting-bundle visualizations are designed to highlight the relation of two crossing neuronal pathways. In the following, visualization methods are proposed which aim at extracting and visualizing important features of both conditions. Details related to the shader pipeline are discussed in Section 5.

4.1. Inner-bundle Visualizations

Inner-bundle visualizations facilitate fiber exploration while at the same time provide understanding of the global bundle shape. Cutaway techniques aim at facilitating insight into an object by clipping parts of the context object or adjusting its transparency. Here, this results in clipping parts of the hull geometry in order to reveal underlying fiber structures.

Three different cutaway approaches were developed, including an either automatic or user-based definition of clipping regions. The *marker-dependent* technique applies a user-defined point of interest and is view-independent. Contrarily, *view-dependent* approaches are defined by the current view and, therefore, adapt due to camera movement. Important spatial as well as functional fiber features are visualized using the proposed color encodings. The following subsections will introduce individual techniques.

4.1.1. Marker-dependent Cutaway

A 3D coordinate determines the center for marker-dependent circular clipping. The user defines a point on the hull's surface through a mouse click on the hull representation as indicated in Figure 3 in the bottom left part. This point defines the origin of the circular hull clipping. The radius of the is adjustable through a slider. This information is transferred as uniforms to the deferred shading pipeline stage in order to compute the binary 3D masking texture. Figure 3 shows a visualization of the resulting marker-based cutaway.
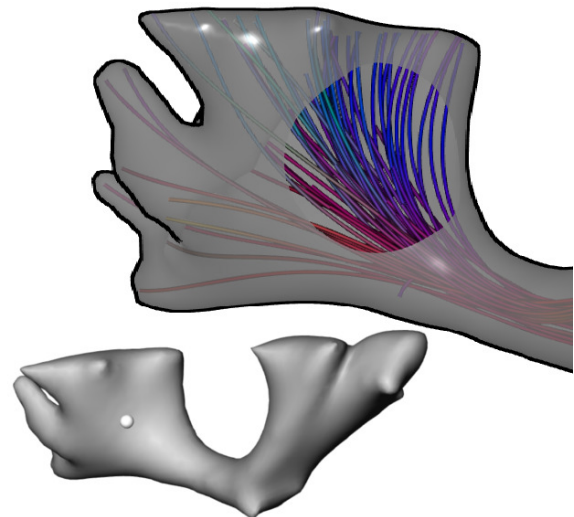

Figure 3: Marker-dependent cutaway visualization: the user places the marker coordinate (bottom left) and adjusts its radius which results in a circular cutout (top right).

4.1.2. View-dependent Cutaway

A further approach computes the cutaway based on the current view. In particular, the circular clipping origin is defined by the viewport center. The user can adjust the radius and radial smoothness of the cut out with immediate feedback. Results of the approach are illustrated in Figure 4.

The second view-dependent cutaway technique computes hull transparency with respect to surface orientation. The idea is to enable a see-through for viewer facing surfaces
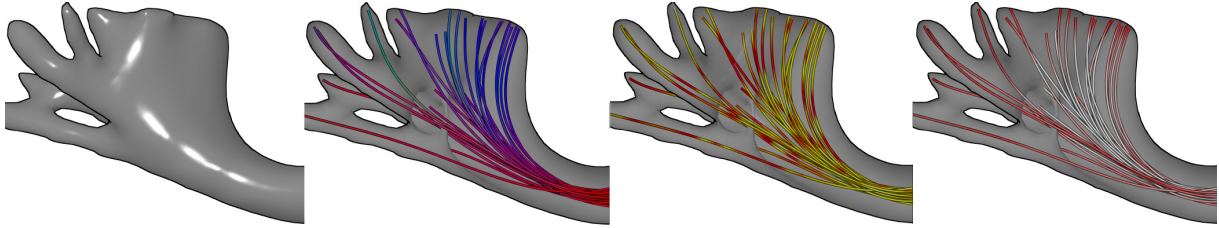
Figure 2: Visualization of fiber color codings: the fiber encompassing hull and view-dependent cutaway renderings reveal inner-bundle fibers. Applied fiber color mappings from left to right: directional color coding, anisotropy color coding (yellow represents high and red low anisotropy), and distance to hull color coding (red indicates fibers in the vicinity of the hull).
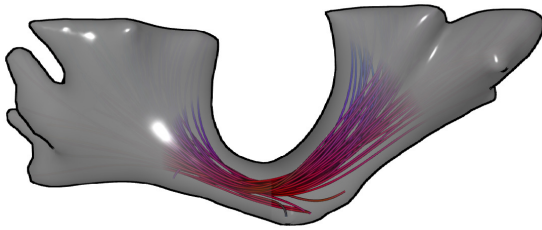

Figure 4: View-dependent cutaway visualization with respect to the viewport center: hull cutout with applied radial smoothness with a small (left) and a large (right) radius.

while providing context information. The dot product by the vertex normal and the view vector is used to estimate surface orientation. A user-defined threshold, implemented as a slider, is used to adjust hull transparency with respect to face orientation. Therefore, hull clipping results in a smooth opacity increase from regions facing the viewer to regions turning away from the viewer. Figure 5 displays a result of the approach for two different thresholds.
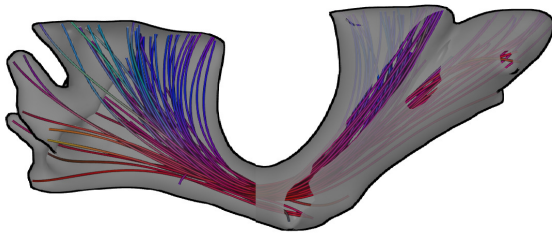

Figure 5: View-dependent cutaway visualization with respect to the view vector: different thresholds are applied to either facilitate underlying fibers (left) or the hull (right).

4.2. Intersecting-bundle Visualizations

HARDI provides detailed information about the spatial relation of neuronal bundles. Therefore, two visualization strate-

gies revealing bundle crossing characteristics were implemented. Two fiber bundles have to be reconstructed and visualized. The first bundle is represented using streamtubes and the second using a fiber encompassing hull.

4.2.1. Intersection Marking

Color encodings and transparency adjustments to the hull's surface are used in order to highlight bundle overlapping areas. Therefore, the fiber encompassing hull as well as the fiber geometry is rasterized in a first step to define overlapping regions. Afterwards, their intersections are defined and transfered to the GPU via a 3D texture. Fragment colors as well as the transparency are adjusted in the fragment shader. Bundle overlapping regions are displayed transparent in combination with an outline of the crossing area. Figure 6 shows results of the proposed intersecting markings for fibers running in the *centrum semiovale*, a region in the brain where the *corpus callosum*, the *superior longitudinal fasciculus*, and the fibers of the *pyramidal tract* meet.
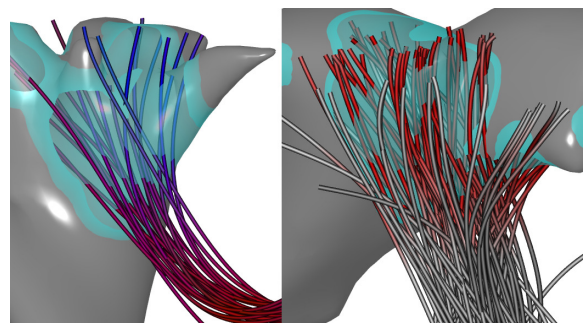

Figure 6: Intersection marking visualization: individual bundles are displayed as streamtubes or a fiber encompassing hulls. Intersections are transparent and overlapping boundaries visualized in light blue. Applied directional color coding for callosal fibers (left) and distance encoding of fibers of the pyramidal tract (right).

4.2.2. Plane Exploration

The plane exploration mode applies a 3D cutting plane for hull clipping. Arbitrarily cross-sectional cut outs can be defined by the user. A simple 3D interaction mode is provided in which the mouse is used to define plane rotation and translation. Bundle parts are divided by the clipping plane to be either exterior or interior. According to this they are displayed either transparent or opaque. The silhouette of the cross-section is displayed in yellow to provide additional spatial understanding. Figure 7 shows the focus and context visualization using the introduced cutting plane.
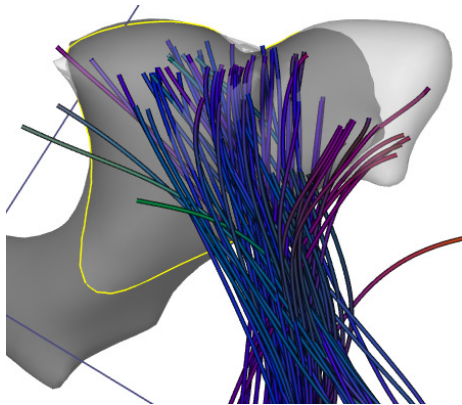

Figure 7: Plane exploration visualization: bundle clipping is defined by an adjustable plane. The outline of the cross-section is displayed in yellow.

5. Workflow and Implementation

The proposed visualization methods were implemented using *MeVisLab* a development environment for medical image processing and visualization [MeV12].

Figure 8 shows an overview of the computation and interaction pipeline. First, fibers are reconstructed based on a user defined seeding region. Afterwards respective hulls are computed. Fibers are at first rendered using a line strip primitive. The subsequent shader pipeline is responsible for generating view-oriented triangle strips. The distance of fiber points to a geometry is computed in the next step for subsequent color mapping. The required geometry is either the corresponding hull of the first or the second bundle or any other geometry. Distances are computed on the CPU before fiber rendering using the winged edges meshes (WEM) representation for hulls. For each fiber point the distance to each WEM node is determined. Attribute variables are used to assign the shortest distance to the respective vertex of the line primitive. Therefore, the information is accessible in subsequent shader pipelines.

The proposed visualizations are realized using a deferred shading approach. Two 2D parameter textures are computed:

The first stores the geometry normals and the second combines necessary scalar information for further visualizations. The fragment depth is stored in the red channel, the marker-defined visibility of the hull is encoded in the green channel, and a flag for hull identification is stored in the blue channel. Additional texture inputs for subsequent compositing are offscreen renderings of the fibers and the hull. Predefined shader pipelines built upon these textures and compute the final cutaway views in an upcoming rendering pass.

Since visualizations are implemented as screen-space approaches, special care has to be taken for cutaway techniques. Here, cutaway renderings aim at revealing fibers as well as hull backfaces. The fragment shader has no information about the scene lying behind the cut outs. To deal with this correctly, we render hull backfaces in the course of the deferred shading approach and make use of the according depth buffer in the compositing stage. In combination with fiber depth information we compare depth values in order to determine the current fragment to belong to either hull or fiber. The left part of Figure 5 shows correct hull backface and fiber rendering.

6. Results and Discussion

In the following, results of the proposed algorithms are presented and discussed. Performance evaluation was accomplished on a Core2 Duo, 3.16 GHz with 4 GB RAM and a NVIDIA GeForce GTX 285 graphics card.

Inner-bundle visualizations provide information about underlying fiber features such as directionality, tightness, anisotropy, or distance to the encompassing hull. Applying color encodings to inner-bundle fibers reveals this spatial and functional information. Figure 2 shows inner-bundle visualizations in combination with a view-dependent cutaway. In the rightmost part, one can clearly identify fiber compartments close to the hull (red). This information is not obtained by simple directional color coding but is important for determining bundle forming fibers. If parts of the hull are subject to clipping the vicinity of fibers to the hull can be estimated through distance color coding. The uncertainty of fiber tracts is a well-known issue in diffusion visualization. The presented inner-bundle characteristics visualizations provide essential information about the reconstruction reliability such as the degree of anisotropy in a certain bundle part. Examination of challenging regions, such as fiber crossings, is feasible through cutaway renderings. In case of false detected fibers, regardless of whether they are of less certainty or belong to a different bundle, they can be removed from the bundle and hulls are recomputed. For a 1024×1024 screen resolution, intra-bundle visualizations are carried out at approximately 80 fps.

Intersecting-bundle visualizations are beneficial for bundle crossing examination. The proposed intersection marking approach highlights bundle overlappings which facilitates spatial understanding. Bundle subsets are displayed
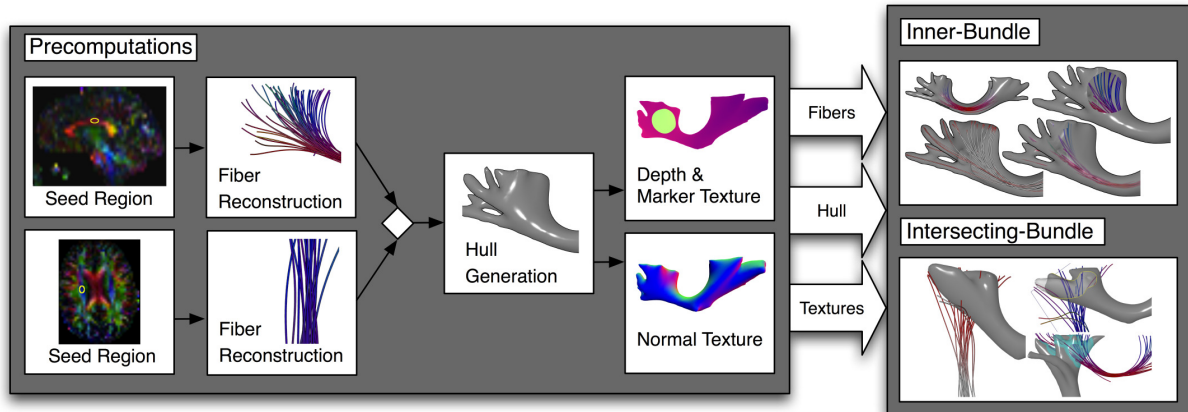
Figure 8: *BundleExplorer* pipeline including preprocessing steps in the right part and visualization approaches in the left part.

transparent within the plane exploration mode. Thereby, insight into regions of interest, such as interwoven bundles, is provided. Distance encodings are interesting in intersecting-bundle visualizations as well. Here, they are applied to reveal the spatial relation between two reconstructed neuronal pathways. Figure 9 shows two different views for two intersecting bundles with applied distance fiber coloring. One can clearly estimate the distance between the fiber and the hull in the right part. However, in the left image the distance is only accessible through color coding. Since the distance
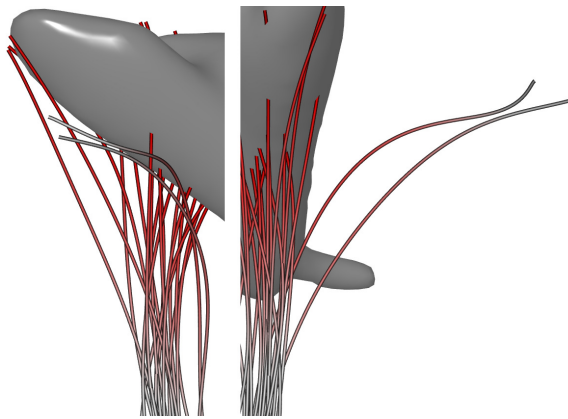

Figure 9: Distance visualization of two intersecting fiber bundles: distance encoding reveals fiber parts far away from the bundle (left) which is proved by scene rotation (right).

assigned to each fiber vertex can be computed from any provided geometry, further scenarios are feasible. For example tumor boundaries are very interesting since spatial relations of neuronal pathways to a lesion are crucial in preoperative planning. Intersecting-bundle visualizations run at approximately 110 fps.

7. Conclusion and Future Work

This paper presents advanced focus and context rendering approaches for complex fiber distributions. They are applicable to diffusion data visualization in general, but specifically focus on problems related to HARDI. The main challenge for HARDI-based fiber visualizations is to consider the visual clutter caused by the intricate nature of neuronal pathways. Conflicting interests in terms of diffusion visualizations exist. Hulls are beneficial in order to hide unnecessary line complexity. However, lines are preferred in some cases since they reveal areas of dense fibers as well as local fiber features. Furthermore, crossing fiber areas can be identified through line representations. In the presented approach we combine both techniques in a user-friendly and intuitive visualization framework and therefore, make a step forward towards complex diffusion data examination.

Several cutaway techniques were presented in this approach. The proposed GPU framework facilitates an easy integration of focus and context rendering approaches. Further cutaways are possible, such as a feature-based: Considering anisotropy classifiers, cut out regions of the hull can be identified by interesting intra-bundle regions such as low anisotropy or crossing fiber pathways. Additional visual enhancements can be integrated in order to further facilitate spatial understanding of line configurations. For example, an illustrative rendering technique for dense fibers was introduced by Everts et al. [EBRI09]. The authors applied depth-dependent halos to emphasize dense line data. The integration of this approach in our framework enhance line interpretation in terms of large fiber bundles. The presented method can further benefit from bundle feature visualization through texture mapping. Eichelbaum et al. [EHHS12] proposed a line integral convolution (LIC) motivated texture visualization for neuronal bundle surfaces which provides tensor analysis. We presented in our previous work [RDMM12a] an intra-bundle raycasting approach coloring the tract sur-

face according to inner diffusion characteristics. Evaluations of both methods, feature visualization for individual fibers and for bundle surfaces, as well as a combination of them is required. Furthermore, the contribution of such approaches to neuroscience research or preoperative planning has to be evaluated.

Acknowledgements

References

[BGKG05] BRUCKNER S., GRIMM S., KANITSAR A., GRÖLLER M. E.: Illustrative context-preserving volume rendering. In *Proceedings of EuroVis 2005* (2005), pp. 69–76. 2

[BHWB07] BEYER J., HADWIGER M., WOLFSBERGER S., B K.: High-quality multimodal volume rendering for preoperative planning of neurosurgical interventions. *IEEE Transactions on Visualization and Computer Graphics 13* (2007), 1696–1703. 2

[DPL*11] DIEPENBROCK S., PRASSNI J.-S., LINDEMANN F., BOTHE H.-W., ROPINSKI T.: Interactive Visualization Techniques for Neurosurgery Planning. *Eurographics (Short Papers)* (2011). 3

[EBRI09] EVERTS M. H., BEKKER H., ROERDINK J. B., ISENBERG T.: Depth-dependent halos: Illustrative rendering of dense line data. *IEEE Transactions on Visualization and Computer Graphics 15* (2009), 1299–1306. 2, 7

[EHHS12] EICHELBAUM S., HLAWITSCHKA M., HAMANN B., SCHEUERMANN G.: Image-space tensor field visualization using a LIC-like method. In *Visualization in Medicine and Life Sciences 2*, Linsen L., Hamann B., Hagen H., Hege H.-C., (Eds.), Mathematics and Visualization. Springer-Verlag, 2012, pp. 193–210. 7

[ESM*05] ENDERS F., SAUBER N., MERHOF D., HASTREITER P., NIMSKY C., STAMMINGER M.: Visualization of white matter tracts with wrapped streamlines. In *IEEE Visualization* (2005), Weikert J., Hagen H., (Eds.), p. 7. 2

[GNBP11] GASTEIGER R., NEUGEBAUER M., BEUING O., PREIM B.: The FLOWLENS: A Focus-and-Context visualization approach for exploration of blood flow in cerebral aneurysms. *IEEE Trans. Vis. Comput. Graph. 17*, 12 (2011), 2183–2192. 3

[KF09] KRÜGER J., FOGAL T.: Focus and context-visualization without the complexity. In *Proceedings of World Congress on Medical Physics and Biomedical Engineering* (2009), Olaf Dössel W. S., (Ed.), Springer, pp. 45–48. 3

[Kin04] KINDLMANN G.: Superquadric tensor glyphs. In *Proceedings of IEEE TVCG/EG Symposium on Visualization* (2004), pp. 147–154. 2

[KSW06] KRÜGER J., SCHNEIDER J., WESTERMANN R.: ClearView: An interactive context preserving hotspot visualization technique. *IEEE Transactions on Visualization and Computer Graphics (Proceedings Visualization / Information Visualization 2006) 12*, 5 (September-October 2006). 3

[MeV12] MEVIS MEDICAL SOLUTIONS AG: MeVis-Lab, medical image processing and visualization. http://www.mevislab.de, June 2012. 6

[MME*09] MERHOF D., MEISTER M., E. B., NIMSKY C., G. G.: Isosurface-based generation of hulls encompassing neuronal pathways. *Stereotactic and Functional Neurosurgery*, 87 (2009), 50–60. 2, 3

[MSE*06] MERHOF D., SONNTAG M., ENDERS F., NIMSKY C., HASTREITER P., GREINER G.: Hybrid visualization for white matter tracts using triangle strips and point sprites. *IEEE Transactions on Visualization and Computer Graphics 12* (September 2006), 1181–1188. 2, 3

[NGE*06] NIMSKY C., GANSLANDT O., ENDERS F., MERHOF D., HAMMEN T., BUCHFELDER M.: Visualization strategies for major white matter tracts for intraoperative use. *International Journal of Computer Assisted Radiology and Surgery 1*, 1 (2006), 13–22. 2

[OVW10] OTTEN R., VILANOVA A., WETTERING H. V. D.: Illustrative white matter fiber bundles. *Computer Graphics Forum 29*, 3 (2010), 1013–1022. 2

[PPAM06] POUPON C., POUPON F., ALLIROL L., MANGIN J.-F.: A database dedicated to anatomo-functional study of human brain connectivity. In *12th HBM Neuroimage* (Florence, Italie, 2006), no. 646. 3

[PPvA*09] PEETERS T. H. J. M., PRČKOVSKA V., VAN ALMSICK M., VILANOVA A., TER HAAR ROMENY B.: Fast and sleek glyph rendering for interactive HARDI data exploration. In *PacificVis* (2009), pp. 153–160. 2

[RDM12] RÖTTGER D., DENTER D., MÜLLER S.: Advanced line visualization for HARDI. In *Bildverarbeitung für die Medizin (BVM)* (2012), Informatik aktuell, pp. 153–158. 3

[RDMM12a] RÖTTGER D., DUDAI D., MERHOF D., MÜLLER S.: Bundle visualization strategies for HARDI characteristics. In *Proceedings of the 8th International Symposium on Visual Computing (ISVC)* (2012). 7

[RDMM12b] RÖTTGER D., DUDAI D., MERHOF D., MÜLLER S.: ISMI: A classification index for high angular resolution diffusion imaging. In *Proceedings of SPIE Medical Imaging* (2012). 4

[RSH05] ROPINSKI T., STEINICKE F., HINRICHS K. H.: Interactive importance-driven visualization techniques for medical volume data. In *Proceedings of the 10th International Fall Workshop on Vision, Modeling, and Visualization (VMV05)* (2005), pp. 273–280. 3

[RSM11] RÖTTGER D., SEIB V., MÜLLER S.: Distance-based tractography in high angular resolution diffusion MRI. *The Visual Computer 27* (2011), 729–738. 3

[TIP05] TIETJEN C., ISENBERG T., PREIM B.: Combining silhouettes, surface, and volume rendering for surgery education and planning. In *EuroVis* (2005), pp. 303–310. 3

[VKG04] VIOLA I., KANITSAR A., GRÖLLER M. E.: Importance-driven volume rendering. In *Proceedings of IEEE Visualization* (2004), pp. 139–145. 3

[VZKL05] VILANOVA A., ZHANG S., KINDLMANN G., LAIDLAW D.: An introduction to visualization of diffusion tensor imaging and its applications. In *Visualization and Image Processing of Tensor Fields*. Springer-Verlag, 2005, pp. 121–153. 2

[WZMK05] WANG L., ZHAO Y., MUELLER K., KAUFMAN A.: The magic volume lens: An interactive focus+context technique for volume rendering. In *Visualization, 2005. VIS 05. IEEE* (2005), pp. 367 – 374. 2